Calibration of X-ray CCDs with an Erect-Field Grating Spectrometer in the 0.2 - 1.5 keV band.

G. Prigozhin, M. Bautz, K. Gendreau[†], G. Ricker

Massachusetts Institute of Technology
Center for Space Research
70 Vassar Str., MA 02139

[†]Goddard Space Flight Center
Greenbelt, MD 20771

July 18, 1996

ABSTRACT

X-ray CCDs developed at MIT Lincoln Laboratories for the AXAF CCD Imaging Spectrometer (ACIS) have been calibrated in the 0.25-1.5 keV spectral range using an erect-field grating spectrometer and an electron impact X-ray source in our laboratory. A combination of the spectrometer with an X-ray CCD on high resistivity substrate allows efficient order separation, and measurement of the CCD energy scale and spectral response function as essentially continuous functions of energy over the spectrometer passband. The CCD energy scale is found to be linear to approximately 0.5% in this spectral band. Relative variations in the detection efficency of the CCD can also be studied with this system. A near edge structure is detected in the CCD response around the oxygen K absorption edge. Comparison of these results with the data acquired with a synchrotron radiation source and monochromator confirms that these structures are features of the detector response. The edge structure allows us to measure the absolute dispersion relation of the spectrometer (and hence the zero-point of the CCD energy scale) with a precision better than 1 eV. We also detect considerable structure in characteristic nitrogen and oxygen emission lines from the electron impact source. We discuss likely mechanisms for the production of this structure.

Keywords: X-rays, charge coupled devices (CCD), X-ray spectrometers, X-ray absorption fine structure (XAFS)

1. INTRODUCTION

The Advanced X-ray Astrophysics Facility[6] (AXAF), being developed as part of NASA's Great Observatories program for launch in 1998, will provide high-angular-resolution imaging spectroscopy and transmission grating spectroscopy in the 0.1–10 keV band. We, together with colleagues at the MIT Lincoln Laboratory and the Pennsylvania State University, are developing the AXAF CCD Imaging Spectrometer[7] (ACIS), one of AXAF's two scientific focal plane instruments. The AXAF mirror assembly and science instruments are being calibrated at the both instrument and system levels. AXAF scientific objectives call for extremely accurate knowledge of instrumental response; for example, the goal for energy scale knowledge accuracy approaches 0.1%.

The ACIS instrument calibration program, summarized in another contribution to these proceedings,[8] includes measurements of the CCD energy scale and spectral response function, as well as absolute measurements of X-ray CCD detection efficiency as a function of X-ray energy and detector position. In this paper, we describe techniques developed to determine the instrumental energy scale and spectral response function at energies below 1.5 keV.

Ten X-ray CCDs will be placed in the focal plane of the ACIS. X-ray CCD technology matured now to the level where spectral resolution is close to the theoretical limits even for big arrays. Each ACIS device has an image section of 1024 x 1024 pixels and is manufactured on a high resistivity (5000 $Ohm \cdot cm$) silicon. A detailed description of the ACIS CCD can be found elsewhere.[1] Both frontside illuminated CCDs and backside illuminated devices will be utilized in the instrument focal plane, and both types of the devices have been calibrated with the technique described below. In this paper, though, we concentrate on the results for the frontside CCDs only. To perform a calibration of these devices in a low energy band from 0.25 to 1.5 keV each device was put into the focal plane of the soft X-ray High Resolution Erect-Field Spectrometer (HIREFS[2]) illuminated by an electron impact X-ray source.

An X-ray CCD coupled with an X-ray spectrometer offers an extremely powerful tool for studying the properties of both CCD and an X-ray source used in the measurement. Emission lines seen in the output spectrum reveal wealth of information about the material of the target of the electron impact source, whereas edges in the spectrum and intensity variations tell a lot about CCD response function. Here we present some results of these measurements.

2. DESCRIPTION OF THE EXPERIMENTAL SETUP

The apparatus used for this experiment consists of an electron impact source, the grating spectrometer (HIREFS), and a CCD chamber (see Fig. 1).

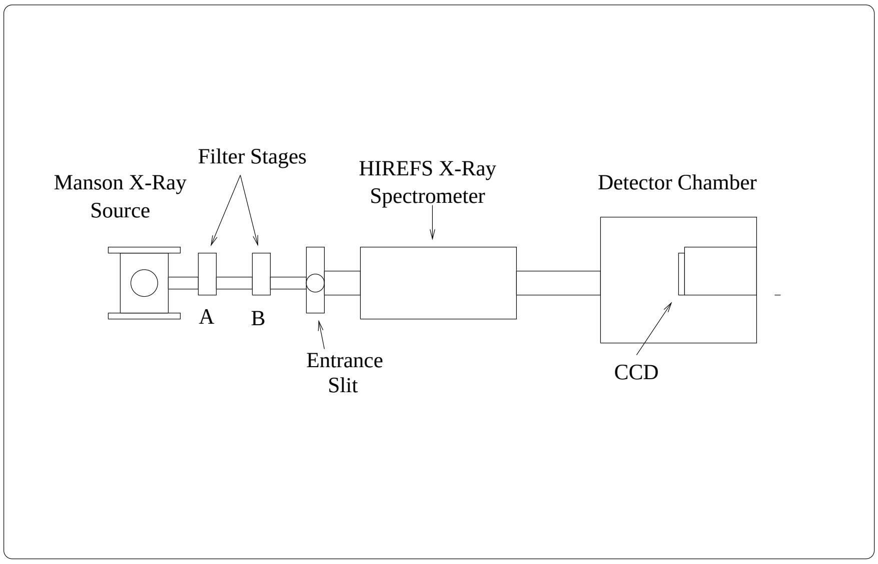

Figure 1: Basic schematic of the calibration setup.

The electron impact source (Manson source) operates at 5 kVolts accelerating voltage and emits bremsstrahlung radiation with energy up to approximately 2 keV. Emitted continuum X-rays pass through filter stages (used to adjust the flux) and narrow (5 microns) entrance slit to hit the reflecting focusing optics and the grating of the spectrometer. Dispersed in the vertical direction, an X-ray beam illuminates a CCD in such a way that every row sees different energy (the CCD columns are parallel to the dispersion direction). In the horizontal direction beam is made wide enough to illuminate every column of the CCD.

The spectrometer has two focusing mirrors and a variable-space reflecting grating, which allows it to produce an erect planar image on the CCD placed normal to the output beam. The spectrometer diffracts multiple orders in any given direction. A tremendous advantage of using a high resistivity X-ray CCD in a combination with a spectrometer is that it allows separation of orders if an X-ray flux is low enough to avoid photon pile up. To illustrate how this has been done, on Fig. 2 is shown a three-dimensional distribution of the number of counts as a function of the CCD row number (x-axis) and a pulseheight (y-axis). Since the dispersion direction of the spectrometer is parallel to the column of the CCD, all the events from the same row have identical energies. The CCD distinguishes the various spectrometer orders into separate ridges in Fig. 2, and, hence, each order can be analyzed separately. Sharp peaks in Fig. 2 correspond to carbon and oxygen emission lines of the source and are due to contamination of the surface of the gold anode by hydrocarbons.

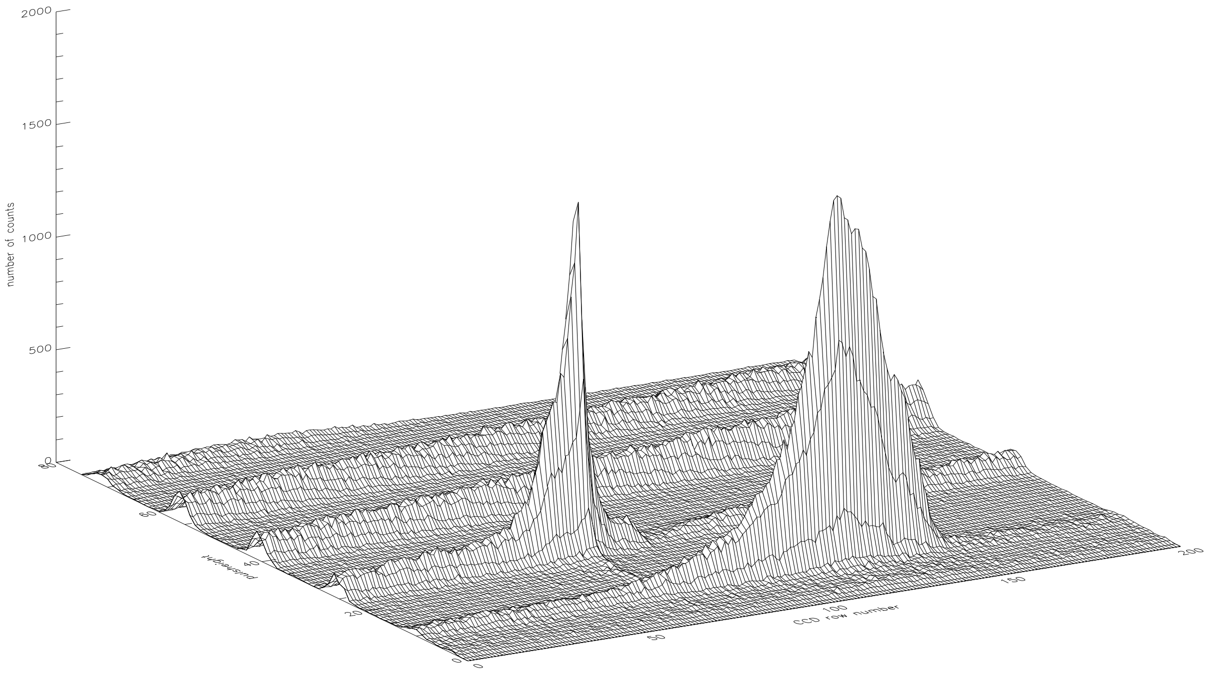

Figure 2: Intensity (number of counts) distribution the X-ray photons as a function of CCD row number (x-axis) and pulseheight (y-axis).

The X-ray flux illuminating the CCD must be maintained at low levels to allow a separate detection of each photon. In order to get a statistically sufficient amount of data we typically collect 5000 frames in each calibration run. During each experiment the CCD temperature is maintained at -120 ± 1.5^0 C to ensure a very low dark current at integration time as long as 7 seconds. The electronics used in this experiment allows computer controlled data acquisition with readout noise normally below 3 electrons rms. For some detectors noise levels below 2 electrons rms are observed.

3. WAVELENGTH SOLUTION

Summing all the counts in each row of the CCD separately for each order of the spectrometer, and plotting intensity as a function of row number, Fig. 3 was produced, only the three first orders are shown.

Fig. 3 shows a result of order separation, or, in other words, plots of intensity as a function of CCD row number for the first three orders of the spectrometer. A number of emission lines can be clearly seen in the spectrum, as

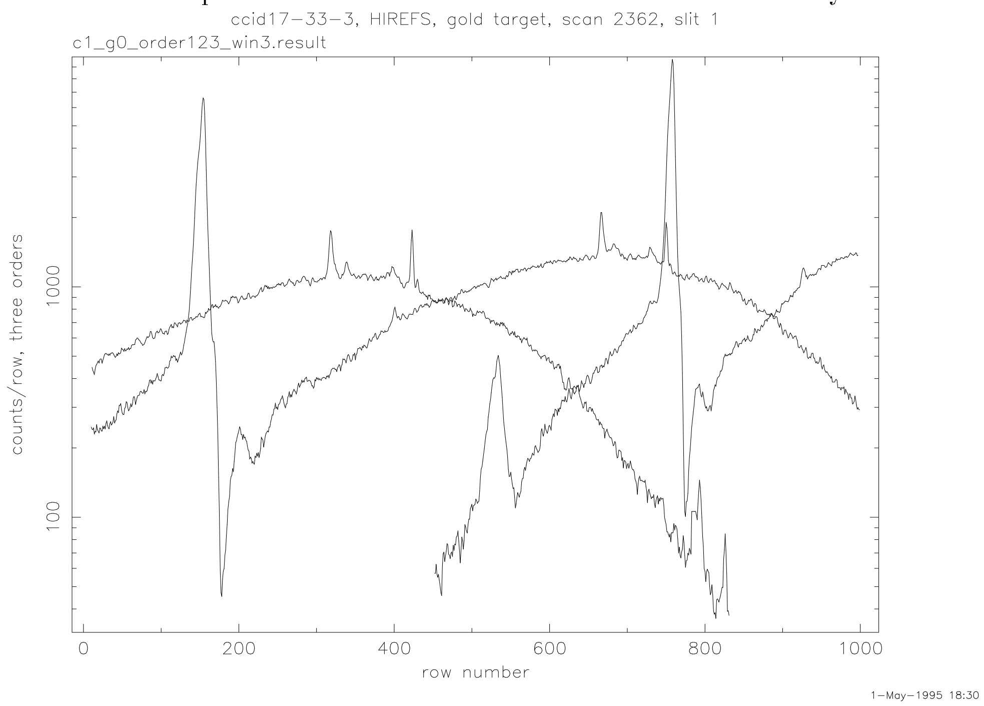

Figure 3: Intensity as a function of row number for three orders of the spectrometer with a gold target in the X-ray source.

well as a very clear absorption edge (presumably, oxygen edge). To convert the results into the energy scale one has to find the correspondence between row number and an energy of the incoming beam. This can be done by solving the grating equation and identifying at least some known emission lines. Fig. 4 shows schematically the geometry of the output stage of the spectrometer and the CCD. The input X-ray beam hits reflecting grating at an angle α and, after being diffracted, a component of wavelength λ illuminates a vertical plane of the CCD at the row x. Angle $\alpha + \beta_c = 2\theta$ is fixed by the spectrometer geometry and by design of the HIREFS, $2\theta = 176^o$.

From Fig. 4 it is clear that

$$\beta - \beta_c = \arctan \frac{(x - x_0) l_{pix}}{L} \tag{1}$$

where $l_{pix} = 24$ microns is CCD pixel size, L is a distance from the grating to the focal plane. From the standard grating equation we have:

$$m\lambda = d \sin\alpha - d \sin\beta \tag{2}$$

Here m is an order number, d is a grating period (208333 $Angstroms$). Converting wavelength λ (in $Angstroms$) into energy E (in keV) with a formula

$$E = \frac{12.399}{\lambda}$$

and combining (1) and (2), we get an equation that determines an energy of the incoming beam as a function of the row number of the CCD:

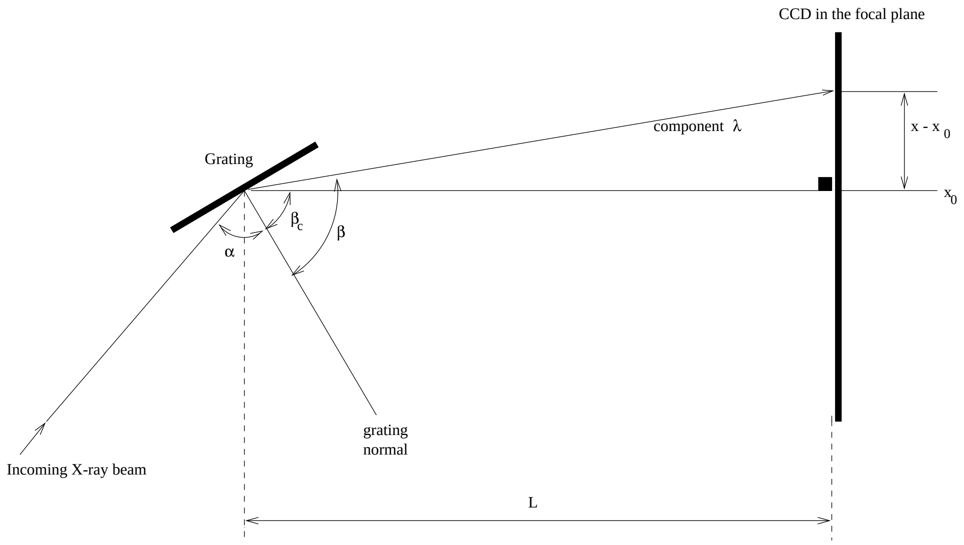

Figure 4: Geometry of light path between the grating and the CCD in the focal plane.

$$E = -m \frac{12.399}{d} \left(\sin\left(\beta_c + \arctan \frac{(x - x_0) l_{pix}}{L}\right) - \sin \alpha \right)^{-1} \tag{3}$$

Angles α and β_c are defined by a geometry of the HIREFS, and if the spectrometer is properly calibrated,

$$\alpha = \theta - \arcsin \frac{m \lambda_c}{2d \cos \theta}; \qquad \beta_c = 2\theta - \alpha. \tag{4}$$

Here λ_c is reading of the wavelength counter of the spectrometer in *Angstroms*, it corresponds to the first order wavelength, hitting CCD at the row x_0.
To set a precise energy scale we use several emission lines with known energies, namely, carbon K_α, nitrogen K_α, and oxygen K_α lines. Both first and second order oxygen line are used in this calibration procedure. The least square fit to the relation (3) with x_0 and L as free parameters at the emission line energies is usually fairly robust. We found that the value of L produced by fitting routine can be used to adjust the distance between the grating and the CCD, if the detector is out of focus. In fact, this is the most precise way to focus the instrument.

Equation (3) allows one to determine a resolving power of the apparatus for any given energy, in the case that it is limited by a detector spatial resolution. The corresponding plot is shown at Fig. 5. Resolving power R here is defined, given the relative difference in energy ΔE seen by two adjacent rows of a CCD, as

$$R = \frac{E}{2\Delta E/row}$$

. For the interval of interest from 0.2 keV and up to 2 keV R changes roughly from 600 to 300.

4. SPECTRAL CURVES

After the row-to-energy relation is established, all results can be plotted as a function of energy. Plots of intensity (number of photons of a given energy seen by the CCD) as a function of energy for the first three orders

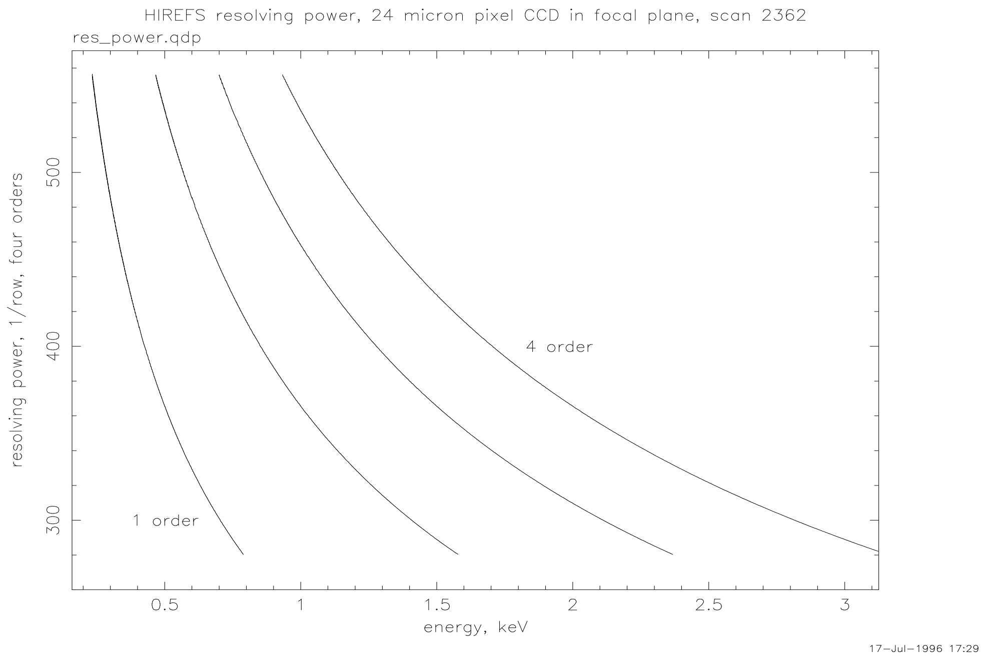

Figure 5: Spectrometer resolving power $\frac{E}{2\Delta E/row}$ as a function of energy.

for a frontside illuminated CCD are shown on Fig. 6. Here the same emission lines in different orders come together, since they have the same energy. They are aligned with an accuracy of better than 0.2 eV.

The data shown on Fig. 6 were taken with the gold target in the X-ray source. The spectrum is dominated by bremsstrahlung radiation with a few emission lines. The strong line at 525 eV is oxygen K_α, weaker ones are nitrogen K_α at 392 eV, copper L_α (930 eV) and L_β (950 eV), and sodium K_α (1041 eV). The origin of all these lines can be explained by the contamination of the surface of the target. A film of hydrocarbons is building up on the surface (this has been confirmed by a separate X-ray photoemission spectroscopy, or XPS, study).

To illustrate the power of this setup as a spectroscopic tool, Fig. 7 shows a spectrum produced by a stainless steel target. Numerous L series of iron, chromium, manganese, and nickel lines reveal a complex composition of the target material. Copper line is a result of the contamination of the target by the material from the hot leads of the filament.

5. CCD LINEARITY AND SPECTRAL RESOLUTION.

An energy scale for the spectrometer illumination pattern has been established using only wavelengths of fiducial lines and geometrical parameters of the CCD (and its ability to separate orders). This implies it is possible to measure the linearity of the CCD response to the X-rays. For each row of the CCD a histogram of the signal pulseheights corresponding to the photons of the given order forms a peak whose shape is close to a gaussian. A gaussian fit was made for these peaks in every row, each order being fitted separately. The centroid of the gaussian is plotted as a function of photon energy in Fig. 8.

To convert output signal into electrons CCD gain was defined at 525 eV (oxygen K_α line), assuming that electron-hole production energy is 3.65 eV. The result looks remarkably linear, especially taking into account that 3 orders are plotted together. A linear fit to these data produces the relation $R = 0.14791 + 1000(1/3.6425)E$,

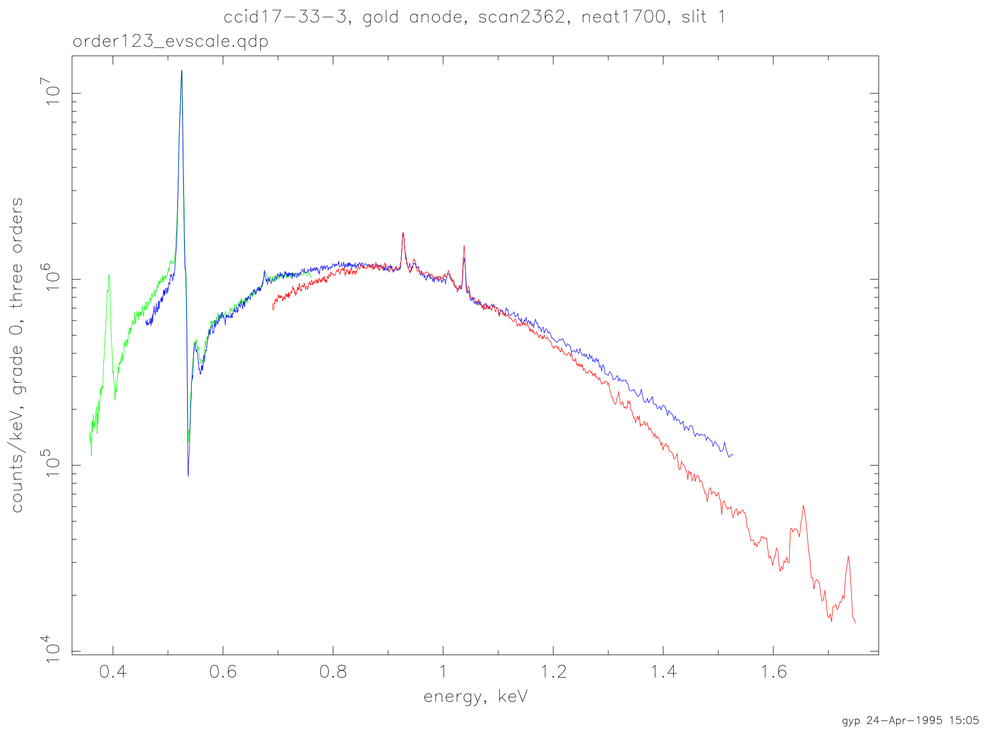

Figure 6: Intensity as a function of energy for three orders of the spectrometer with a gold target in the X-ray source.

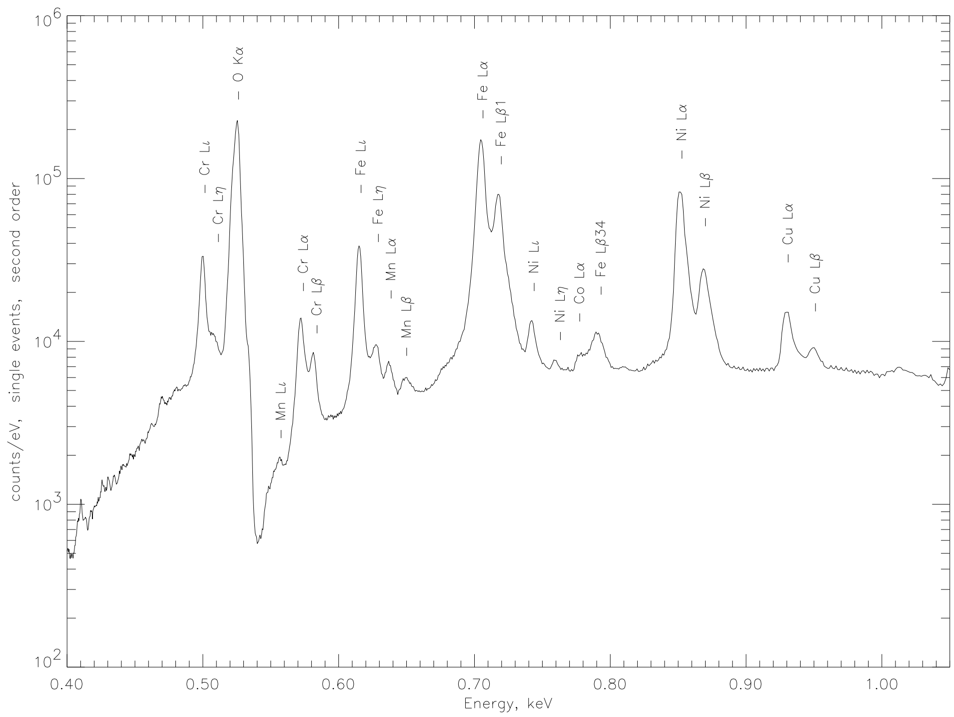

Figure 7: Intensity as a function of energy, second order, stainless steel target.

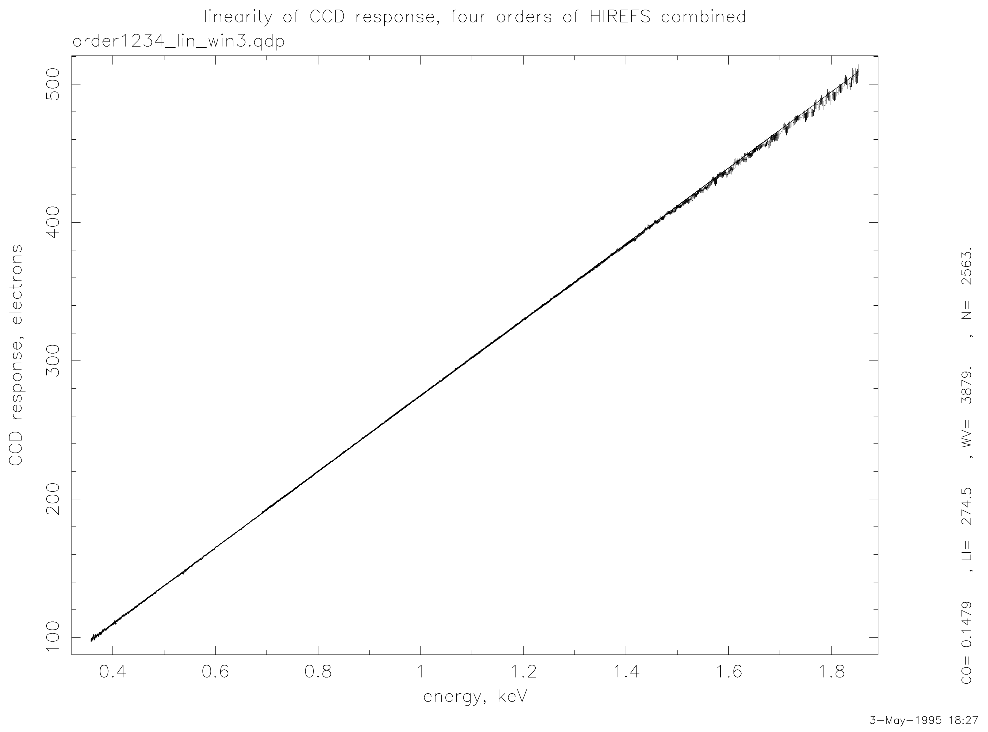

Figure 8: CCD response (peak center) as a function of energy.

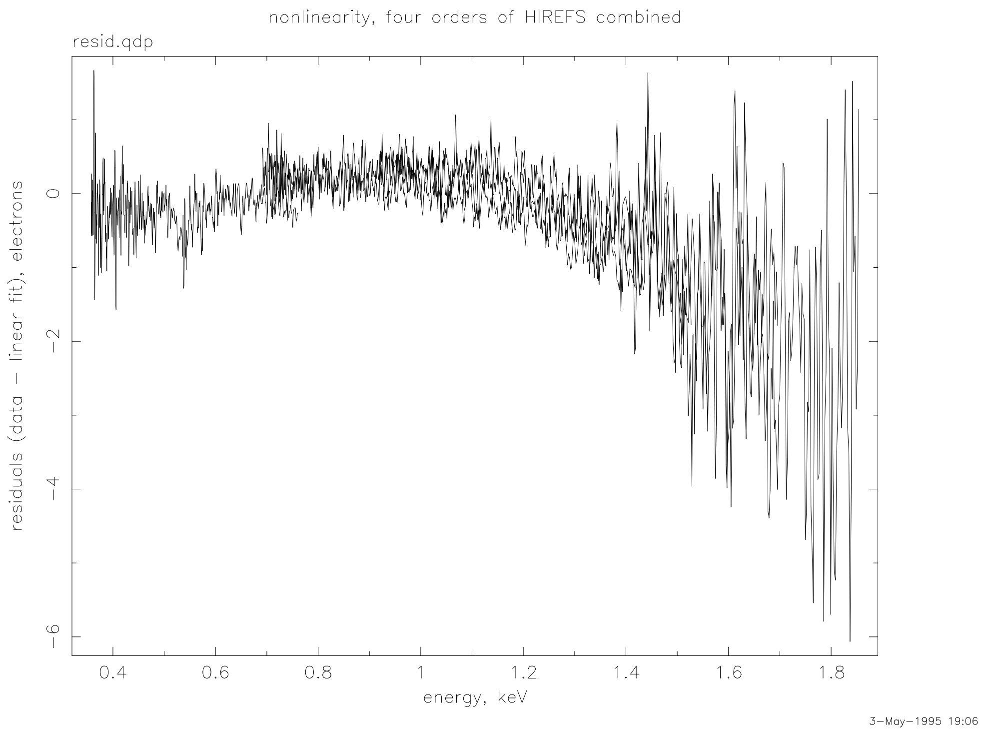

Figure 9: CCD response (peak center) as a function of energy.

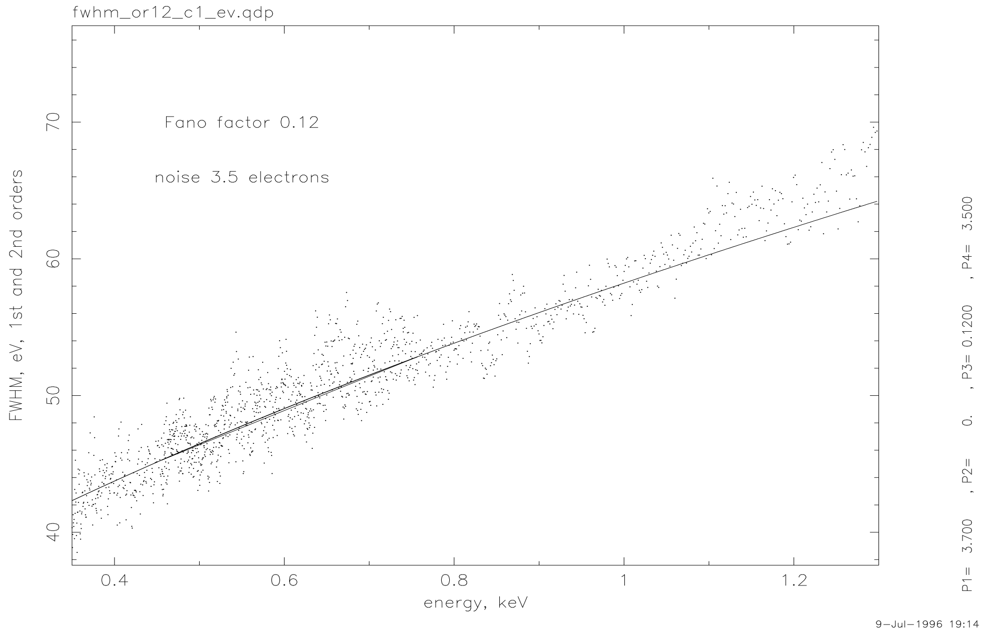

Figure 10: CCD energy resolution (FWHM) as a function of energy.

indicating that an offset from zero is less than 0.15 electrons. On Fig. 9 is shown the difference between data points and the linear function $R(E)$. As it can be seen, for most of the data residuals are within the range of ± 1 electron from zero. At higher energies CCD response starts to fall slightly below the linear approximation, although even at 1.8 keV a the deviation is still within 1%. One possible explanation of the nonlinearity is that charge collection efficiency declines slightly at higher energies as the charge cloud size becomes bigger.

Another useful result of making a gaussian fit to the pulseheight distribution in each row of the CCD is a plot of spectral resolution (a gaussian full width at half maximum) as a function of energy shown on Fig. 10. A theoretical prediction for this plot (solid line) is described by a formula:

$$FWHM = 2.35 \times \epsilon \sqrt{N^2 + \frac{EF}{\epsilon}}$$

where ϵ is an energy required for one electron-hole pair creation (3.65 $eV/pair$), $F = 0.12$ is the Fano factor, N is rms readout noise in electrons, and E–photon energy. The data points follow the theory reasonably well.

6. OXYGEN ABSORPTION EDGE AND EMISSION LINES STRUCTURE.

The CCD gate structure contains layers of silicon dioxide to isolate the gates from the substrate as well as to separate different clocks from each other.[1] This implies a complicated X-ray response at energies close to the oxygen K_α absorption edge. A close look at the spectrum in the vicinity of the oxygen edge (see Fig. 11) reveals a pronounced structure right above oxygen absorption edge at 536 eV. The edge energy is found to be different from the tabulated value of oxygen edge, namely, 543 eV.[9] The shift of the energy is caused by a different energy of the Si–O bond, compared to the energy of the double bond in the O_2 molecule, whose energy is given in the cited above table. These intensity variations represent so-called X-ray Absorption Fine Structure (XAFS[4]) and are caused by the backscattering of the electron wave function from the atoms surrounding the

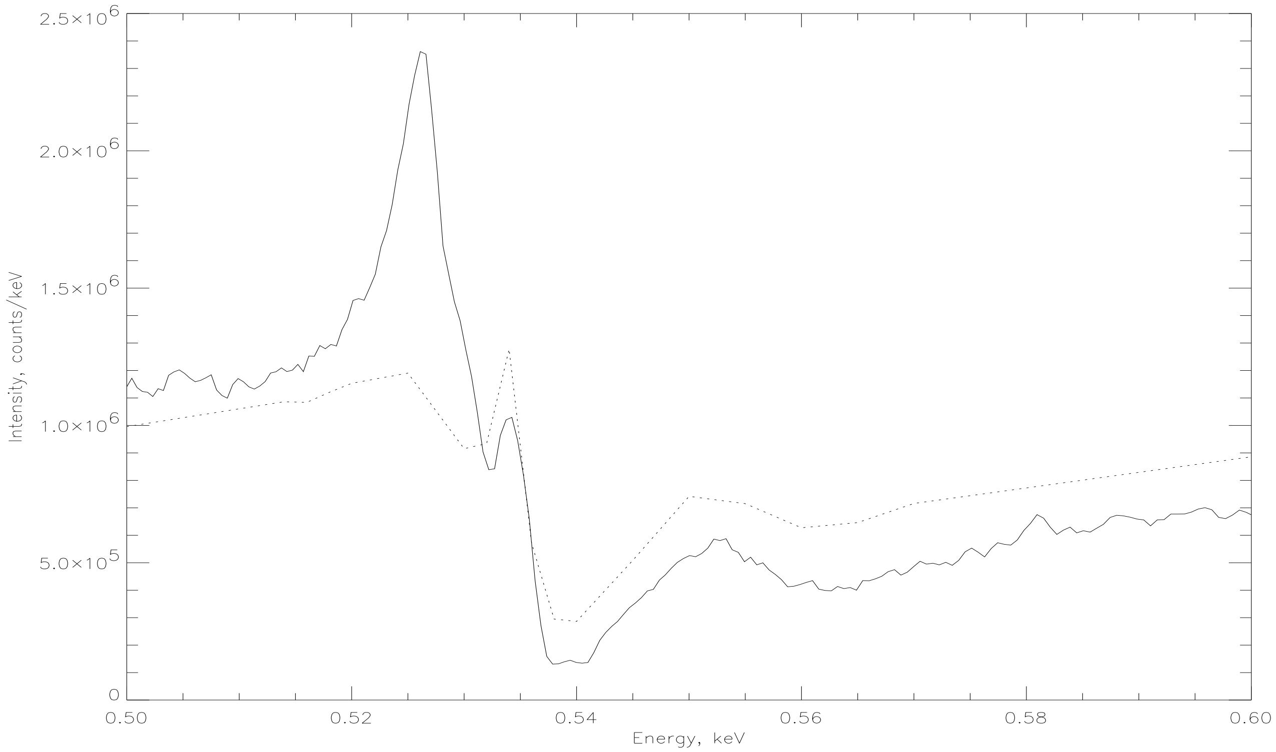

Figure 11: Intensity as function of energy in the vicinity of the oxygen edge (solid line). Dotted line represents QE plot of the CCD multiplied by a factor of 4×10^6 to match the scale.

one which interacts with the incoming X-ray photon. The increase in the absorption right above oxygen edge is significant and shows a big dip at 540 eV. This feature is very obvious in both Fig. 6 and Fig. 7. The dotted line on Fig. 11 represents a scaled quantum efficiency plot for the device, the measurement being performed at a synchrotron with a calibrated reference detector. The absolute detector efficiency measurements were performed at the PTB laboratory at BESSY, and will be described elsewhere.[3] Here we plot the synchrotron results merely to illustrate the reliability of features observed with the HIREFS. The HIREFS intensity plot exhibits the same XAFS oscillations as the synchrotron data; even the sharp peak on the low-energy side of the edge is reliably reproduced. This is an excellent check of the energy scale of the HIREFS, since two measurements are completely independent and the accuracy of the energy scale of the SX700 monocromator used at the synchrotron facility is better than 0.7 eV.[5]

Thus the HIREFS can be used to reveal XAFS structure in the CCD response with very fine energy steps. The oxygen edge in the HIREFS data is stronger than the QE plot predicts. This fact suggests that some part of the edge in the HIREFS data comes from the X-ray source, and is not entirely being produced be the CCD. Evidently film of hydrocarbons forms on the surface of the target in the X-ray source containing oxygen, nitrogen and carbon. Emission lines from all these elements are excited by the electron beam and are observed in the output spectrum. At the same time, oxygen contained in the film produces an edge in the spectrum, in addition to the edge produced by the SiO_2 in the CCD gate structure. To make a measurement of the oxygen absorption edge of the CCD it is very important to keep an intensity of the oxygen K_α line (525 eV) emitted by the source, as low as possible. For that reason a gold target was used in these experiments. The gold target does not eliminate oxygen line entirely, but produces much better results than any other target we have tried. We were able to reduce oxygen line intensity to a very low level (see Fig. 11) by keeping an electron emission current at high levels, thus increasing target temperature. The observed line intensity is about the same as the intensity of the underlying continuum.

The emission lines of all three light elements seen in the spectrum – carbon, nitrogen and oxygen – have a distinct double-peaked structure. This structure is very obvious in Fig. 2 even without making functional fits to the spectrum. More detailed quantitative analysis shows that the oxygen line consists of the wider ($\sigma = 1.3$ eV) line at 525.0 eV, and a sharper component ($\sigma = 0.9$ eV) at 526.6 eV. The nitrogen line appears to be a combination of the peaks at 392.0 eV ($\sigma = 3.8$ eV) and 395.0 eV ($\sigma = 2.6$ eV). The carbon line structure is even more complicated, showing peaks at 277.0 and 279.0 eV, as well as few other not so clearly defined peaks at higher energies. The splitting of the lines is caused by chemical shifts of the energy levels. An XPS study clearly identifies at least two types of bonds: C–C and C–O, which explains the complicated structure of carbon line. It is also very likely that difference between energy levels of σ and π types of molecular orbitals is responsible for splitting of the oxygen and nitrogen lines. This is a subject of further investigation, which can potentially improve an accuracy of the energy scale of the spectrometer.

7. CONCLUSIONS

A combination of an X-ray CCD and a grating spectrometer in addition to being a very powerful spectroscopic tool allows to calibrate CCD linearity and energy resolution in a low energy band. CCD response is found to be linear to approximately 0.5% below 1.5 keV. The setup also reliably detects near edge absorption structure without using an expensive and hardly accessible syncrotron source.

8. ACKNOWLEDGMENTS

This work was funded by the NASA AXAF program.

9 REFERENCES

[1] B. E. Burke, R. W. Mountain, P. J. Daniels, M. J. Cooper, V. S. Dolat, CCD soft x-ray imager for ASCA and AXAF, Proc. SPIE, vol. 2006, pp.272-285 (1993)

[2] M. Hettrick, US Patent No. 4,776,696

[3] G. Prigozhin et al., Absolute Measurements of Oxygen Edge Structure in the Quantum Efficiency of X-ray CCDs. To be published.

[4] B. K. Teo. EXAFS: Basic Principles and Data Analysis, Springer-Verlag, 1986

[5] F. Scholze, M. Krumrey, P. Muller, D. Fuchs, Plane grating monocromator beamline for VUV radiometry, Rev. Sci. Instrum. 65(10), October 1994, p. 3229

[6] M. Weiskopf, S. O'Dell, R. Elsner, L. Van Speybrock, Proc. SPIE, vol. 2515, p.312 (1995)

[7] G. Garmire, G. Ricker, M. Bautz, B. Burke, D. Burrows, S. Collins, J. Doty, K. Gendreau, D. Lumb, J. Nousek, Proc. AIAA Space Programs and Technology, March 1992, Huntsville, Al.

[8] M. Bautz, S. Kissel, G. Prigozhin, S. Jones, T. Isobe, H. Manning, M. Pivovaroff, J. Woo, X-ray CCD calibration for the AXAF CCD imaging spectrometer, These Proceedings

[9] B. Henke, E. Gullikson, J. Davis, Atomic Data and Nuclear Data Tables, v. 54, No. 2, July 1993